Miscibility and kinetics of phase separation in polymer blends of tetramethyl-bisphenol-A polycarbonate and polystyrene

W. Guo and J. S. Higgins*
Department of Chemical Engineering and Technology, Imperial College, London SW7 2BY, UK
(Received 31 March 1989; accepted 3 July 1989)

In this paper we report the phase boundaries of tetramethyl-bisphenol-A polycarbonate with polystyrene of different molecular weights, determined using light scattering techniques as well as microscopic methods. The early stages of spinodal decomposition were observed at several temperatures. Analysis of the data using the Cahn–Hillard theory showed that this theory is not able to quantitatively predict the early stages of spinodal decomposition for this blend. Inclusion of thermal fluctuation effects appears to be necessary.

(Keywords: tetramethyl-bisphenol-A polycarbonate; polystyrene; spinodal decomposition; thermal fluctuation)

INTRODUCTION

During the past few years studies of polymer miscibility and the kinetics of phase separation have been a very active field. Several books[1,2] and many papers[3–8] have been published. The miscibility of polystyrene with tetramethyl-bisphenol-A polycarbonate (TMPC) was first reported by Shaw[9] who observed features which suggested lower critical solution temperature (LCST) behaviour. In a more extensive study Casper and Morbitzer[10] established a complete phase diagram for this system. Yet again, by using d.s.c. and other thermal analysis techniques a complete cloud point curve was established and LCST behaviour was noted. Yee and Maxwell[11] reported results of d.s.c. measurements, density and dynamic mechanical measurements for this blend. Similar measurements were also made by Fernandes *et al.*[12]. In a study of neutron scattering from this system Brereton *et al.*[13] reported some rather unusual behaviour of the interaction parameter between the two components, which they interpreted as arising from a spatial structural effect in the system.

In this paper we have obtained phase boundaries of TMPC with polystyrene of different molecular weights using light scattering techniques as well as microscopic methods. The early stages of spinodal decomposition were observed at several temperatures, and comparison made with the predictions of Cahn–Hillard theory.

THERMODYNAMICS OF POLYMER BLENDS

From the Flory–Huggins lattice model[14] the free energy of mixing, ΔG_m for a polymer blend may be calculated as

$$\Delta G_m/RT = n_1 \ln \phi_1 + n_2 \ln \phi_2 + \phi_1\phi_2\chi_{12} \quad (1)$$

Here ΔG_m is expressed per lattice segment and n_1, n_2 are the molar numbers of polymer 1 and polymer 2, respectively. ϕ_1 and ϕ_2 are the volume fractions of the components. x_{12} is the interaction parameter.

Although x_{12} was assumed to be independent of concentration and inversely dependent on temperature in the original Flory–Huggins theory[14], an empirical temperature and concentration dependence has frequently been required to describe behaviour in real systems.

In the diagram *Figure 1* shows a typical dependence of ΔG_m on ϕ_2 for a system which is miscible at the temperature of observation, T_o, and the corresponding miscibility limits in temperature and composition.

As we see clearly, for any composition between ϕ_1 and ϕ_2, the system can reduce ΔG_m by separating into two phases with composition ϕ_1 and ϕ_2. The solid line in diagram b is called the binodal and is defined by the points of common tangent of ΔG_m. At these compositions the chemical potential μ_1 and μ_2 are equal and two phases can coexist.

The dashed line is the spinodal, defined by the points of inflexion where $\partial^2(\Delta G_m)/\partial\phi_2^2 = 0$. These points are ϕ_1' and ϕ_2' in diagram a. For compositions between ϕ_1' and ϕ_2', $\partial^2(\Delta G_m)/\partial\phi_2^2 < 0$ and the system is unstable to all small concentration fluctuations. The phase separation process is called spinodal decomposition. Between ϕ_1 and ϕ_1' and ϕ_2 and ϕ_2' $\partial^2(\Delta G_m)/\partial\phi_2^2 < 0$ so that small fluctuations are damped out and phase separation can proceed only by a nucleation and growth process.

CAHN–HILLARD THEORY

Cahn and Hillard[15] derived a diffusion equation for a spinodal decomposition process

$$\frac{\partial\phi}{\partial t} = M\frac{\partial^2 G}{\partial\phi^2}\nabla^2\phi - 2MK\nabla^4\phi + \text{nonlinear terms} \quad (2)$$

where M is the diffusional mobility of the system and the term K arises from the free energy in the concentration

* To whom correspondence should be addressed

0032-3861/90/040699-08

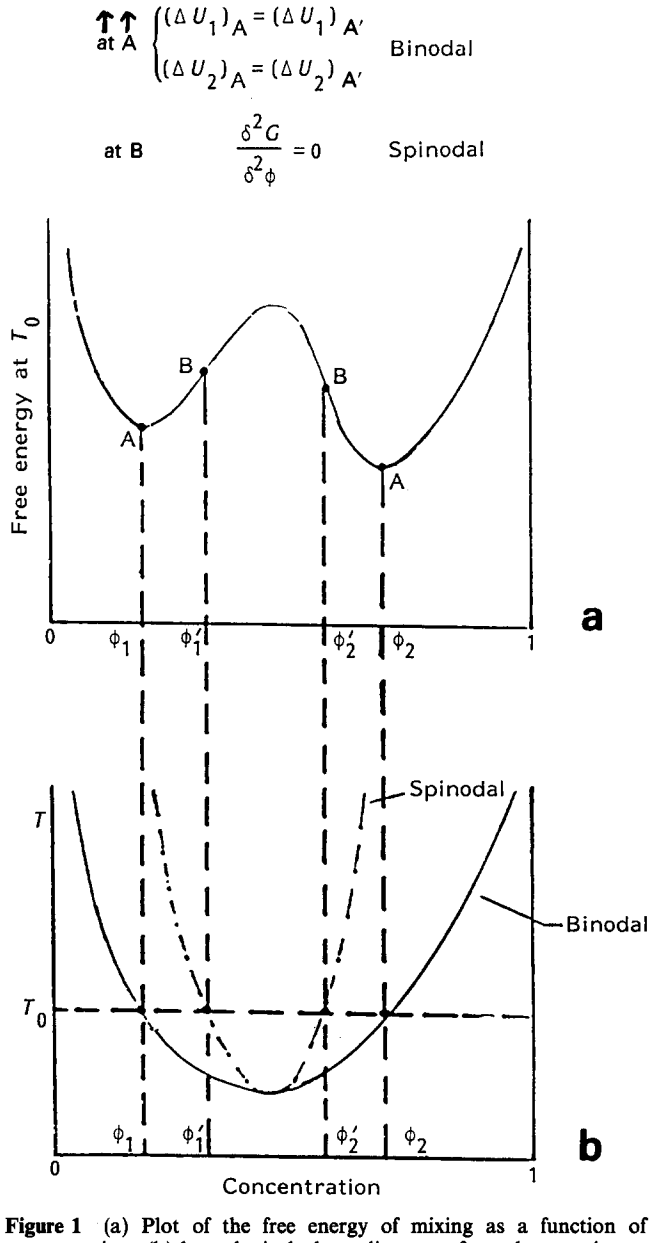

Figure 1 (a) Plot of the free energy of mixing as a function of concentration; (b) hypothetical phase diagram of a polymer mixture exhibiting a LCST

gradients and can be determined[16] from the statistical segment length of the component polymers.

If nonlinear terms are ignored equation (2) can be solved in terms of the growth $R(Q)$ in amplitude, of each Fourier component of the concentration fluctuations.

$$R(Q) = -M\frac{\partial^2 G}{\partial \phi^2}Q^2 - 2MKQ^4 \qquad (3)$$

The function has a maximum at

$$Q_m = \frac{1}{2}\left[-\frac{\partial^2 G}{\partial \phi^2}\Big/ K\right]^{1/2} \qquad (4)$$

and for values of $Q > Q_c$ $(=2^{1/2}Q_m)$, $R(Q)$ becomes negative so that short wavelength fluctuations are damped out.

The scattered intensity from such a system grows exponentially with time as:

$$S(Q,t) = S(Q,0)\exp[2R(Q)t] \qquad (5)$$

Comparing equation (2) with the normal diffusional equation $(\partial\phi/\partial t = D\nabla^2\phi)$ the coefficient of the first term on the right-hand side of equation (2) is identified as the Cahn–Hillard diffusion coefficient D_{app}.

The early stages of spinodal decomposition are observed as an exponentially increasing scattered intensity which develops a maximum at Q_m. During the early stages Q_m is not time dependent. D_{app} can be obtained from the intercept of a plot of $R(Q)/Q^2$ *versus* Q^2 following equation (3). These values extrapolate to zero at the spinodal temperature where $\partial^2 G/\partial\phi^2 = 0$.

EXPERIMENTAL

Materials

The materials used in this study and their characteristics are listed in *Table 1*. TMPC is a thermoplastic with a rather high glass transition temperature and good resistance to hydrolysis. It has the following molecular structure.

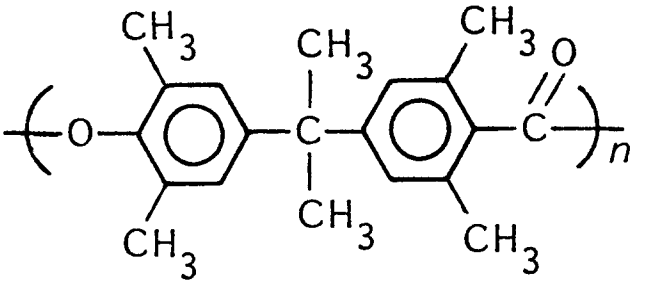

Blend preparation

Methylene chloride ($MeCl_2$) was used as a common solvent for casting films from solution, although benzene can also be used. Several drops of 5% (w/v) solution of a mixture were placed on a cover slip. In order to obtain films with the same thickness the same number of drops was applied to each cover slip. Films with different thicknesses were obtained using different concentrations of solutions. The cast films were left at room temperature until most of the solvent was evaporated. Then they were placed in vacuum oven for 12 h at 80°C and 140°C for 24 h. The dried films were kept in the vacuum oven until used. The film thickness was obtained by measuring the thickness of the cover slip before casting and when the film was dried.

Determination of glass transition temperatures

The glass transition temperatures of the blends were measured using the Perkin-Elmer DSC2. For each blend approximately 10 mg samples were placed in the aluminium pan and heated at a rate of 20°C/min. In all the cases a good agreement was observed in the T_g values for several runs. T_g was arbitrarily determined as that temperature at which the change in the heat capacity

Table 1 Sample characteristics

Sample	M_w	M_n	M_w/M_n	T_g (°C)
TMPC	5.26×10^4	1.79×10^4	2.94	200
PS-3	3.18×10^5	1.36×10^5	2.34	99
PS-5	2.89×10^5	1.13×10^5	2.56	99
PS-7	1.02×10^5	6.37×10^4	1.60	99

[a] The molecular weight values of TMPC are PS equivalent

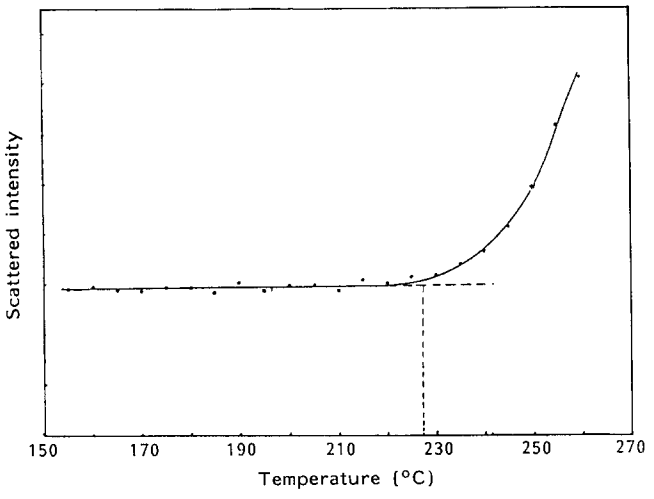

Figure 2 A typical cloud point transition obtained using the light scattering equipment

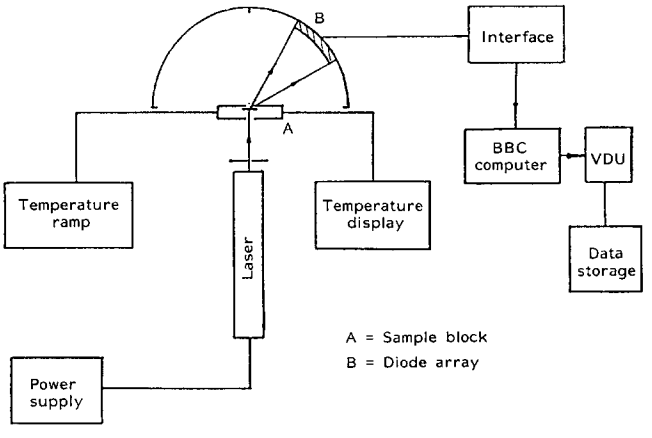

Figure 3 Schematic illustration of the light scattering instrument

over the transition reached half its maximum value (see *Figure 4*).

Determination of phase boundaries

Prior to any studies of real time kinetics the cloud point curves were obtained using the hot stage microscope (Olympus, BH) and light scattering equipment. For the microscopic measurements the sample was placed in the hot stage at a pre-determined temperature for 30 min and then taken out for observation under the microscope. The pre-determined temperature was increased by 5°C each time. This procedure was repeated until a temperature was found at which the mixture just started to phase separate. For light scattering measurements a film sample was placed in the sample block and heated at chosen rates (1.6°C/min, 0.8°C/min, 0.4°C/min). The scattered light intensity was recorded with temperature. The onset of the dramatic increase of the scattered intensity was taken as the cloud point. *Figure 2* shows a typical plot of this kind.

Kinetic experiments

Kinetic experiments were performed using light scattering equipment which was built in our laboratory. The equipment is schematically shown in *Figure 3*. The details of the equipment can be found elsewhere[17]. Basically it consists of a 5 mW He–Ne laser (Aerotech Ltd, UK), a sample block and a light detecting system. The vertical laser beam, after passing the sample which is held at a temperature above the cloud point, is scattered over a range of angles. The wave vector of scattering can be calculated using $Q=4n\pi \sin\frac{\theta}{2}/\lambda$ (n is the refractive index of the mixture, λ is the wavelength of the laser and θ is the scattering angle. In this case $\lambda=6832$ Å). The scattered light intensity is detected using a photodiode array mounted over 60° with 2° intervals. The photodiode array was connected through a multichannel A/D converter to a BBC computer. A program written in BASIC was used for the collection of the data.

In the experiments dried films with a thickness of about 0.3 mm were preheated at 230°C for 30 min and then quickly transferred into the sample block. The temperature of the sample block was controlled at the phase separation temperature with an error of ±0.5°C. From our preliminary experiments some effect of the pre-heating temperature on the subsequent phase separation behaviour was noticed. Therefore, the pre-heating temperature in the experiment was carefully controlled within an error of ±2°C. In order to prevent PS from degradation at high temperatures N_2 was introduced in the sample block at a controlled flow rate. The time needed to reach the phase separation temperature from 230°C was estimated to be about 20 s for a temperature jump of 10°C. From the experimental data the region between 20 s and 100 s was taken as the early stages of spinodal decomposition. The data were analysed using a Fortran program on an IBM-PC.

RESULTS

Glass transition temperatures of the mixture

Figure 4 shows the plots of glass transition temperatures of the mixtures. For all the mixtures tested, a single intermediate T_g is observed as has been seen by other authors[9–11]. This again indicates the miscibility of these two polymers. The values of T_g in the blend can be predicted using the Fox equation[18] written as:

$$1/T_g = w_1/T_{g1} + w_2/T_{g2} \quad (6)$$

where T_g is the glass transition temperature of the blend, T_{gi} are the glass transition temperatures of the

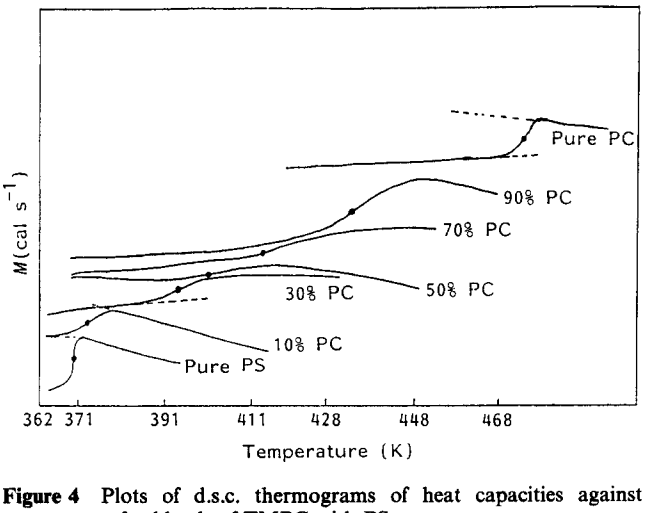

Figure 4 Plots of d.s.c. thermograms of heat capacities against temperature for blends of TMPC with PS

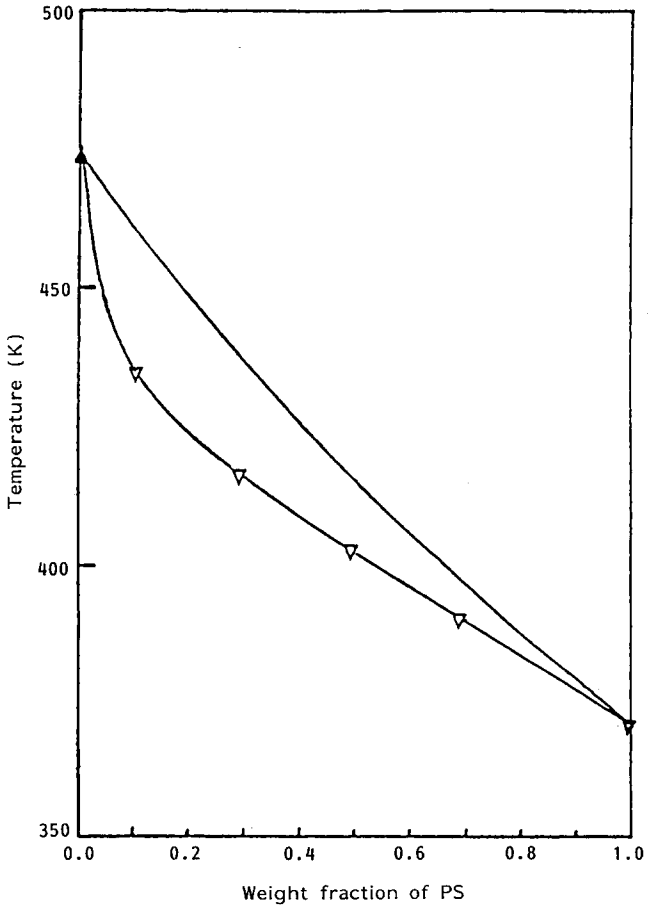

Figure 5 Plots of glass transition temperature of TMPC/PS-5 mixtures. The solid curve is plotted according to the Fox equation; △, experimental results

components and w_i are the weight fractions of the components.

These values are plotted together with the experimental values in *Figure 5*. The theoretical values fall below the experimental ones indicating the invalidity of the Fox equation for prediction of T_g values of these miscible polymer blends. Lower experimental values than those predicted by equation (6) may suggest some kind of special interactions between the two components[1].

Cloud point curves

Effect of heating rates. Because polymers are highly viscous molecules with small diffusional coefficients, the cloud points are very much dependent on the heating rate used in the experiment. This effect is shown in *Figure 6* for the mixture of TMPC/PS-5 (50/50). Clearly the cloud points increase almost linearly with the increasing heating rates tested. By extrapolation the cloud point at isothermal condition (zero heating rate) may be obtained and the resulting temperature is in good agreement with the one determined by microscopic methods (235°C) and by kinetic methods (233°C in *Figure 14*).

Effect of film thicknesses

The effect of film thicknesses on the cloud points for the TMPC/PS-3 mixture is shown in *Figure 7*. As seen in the plot, with increasing film thickness, the cloud point decreases dramatically at first and then levels off. This effect may be caused by the closeness of the refractive indexes of the two components (TMPC, $RI = 1.608$; PS, $RI = 1.59$), i.e. a significant signal can only be achieved with a thicker film.

Effect of molecular weights

Figure 8 shows the effect of molecular weights of PS on the cloud points. Owing to the degradation of PS at temperatures above 270°C the extremes of molecular weights of PS were not used. It was noticed that the molecular weights of PS in the range tested have very small effect on the cloud points. This may suggest that entanglements between different chains are involved to such an extent that they have hindered the phase separation process, although phase separation is favoured on thermodynamic grounds.

Real time kinetics studies

Figure 9 shows the evolution of the scattered intensity from a TMPC/PS-5 (50/50) sample after a temperature jump into the two phase region. In the early stages of spinodal decomposition intensity increases over the whole Q-range, but eventually a maximum appears as predicted by equations (3)–(5). The growth rate of the scattered intensity is exponential at each Q-value in the early stages and a typical plot of intensity *versus* time is shown in *Figure 10*. The data corresponding to *Figure*

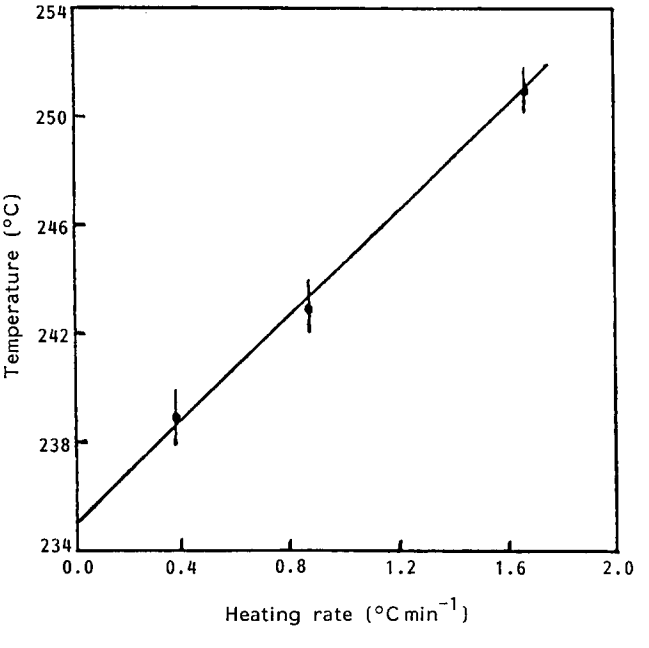

Figure 6 Effect of heating rates on the cloud points of TMPC/PS (50/50) mixture

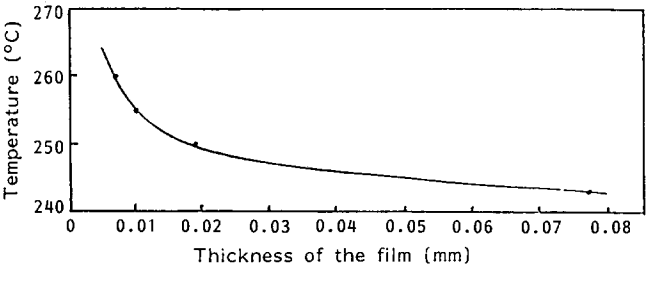

Figure 7 Effect of film thicknesses on the cloud points of the TMPC/PS (50/50) mixture

10 are plotted as ln I *versus* time in *Figure 11*. The linearity of such a plot is usually taken as a sign that the early stages of spinodal decomposition have been observed and that Cahn–Hillard theory[15] would be expected to apply.

In the later stages of the phase separation a marked decrease of the scattered intensity is observed (*Figure 10*). This is caused both by the decrease of the transmitted intensity, because in this stage the sample has become very cloudy, and by the shift of the peaks towards smaller wave vectors.

From the initial slope of the ln I *versus* time plot values of the growth rate $R(Q)$ can be obtained. In *Figure 12* $R(Q)$ is shown as a function of Q at different temperatures. A maximum is observed at Q_m as predicted by equation (5). Some temperature dependence of Q_m can be seen from this plot and in *Table 2*. The initial domain size is calculated as $D_0 = 2\pi/Q_m$.

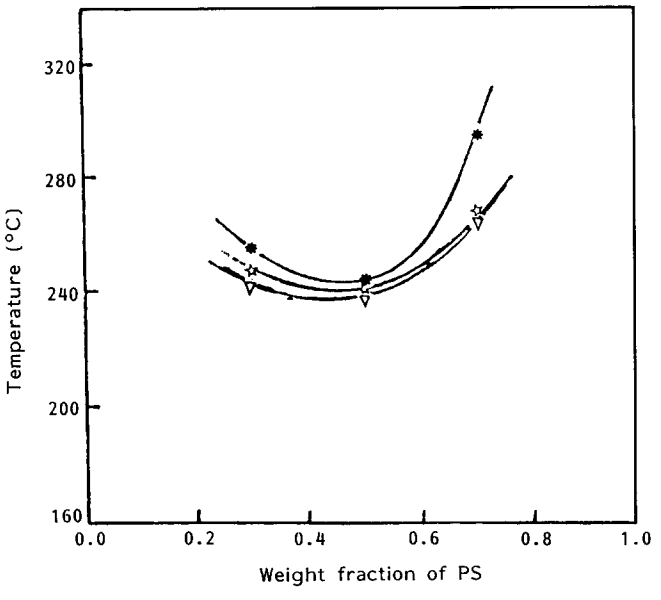

Figure 8 Cloud point curves for TMPC/PS mixtures with different molecular weights of PS, determined by using the light scattering technique. ▽, PS-3; ☆, PS-5; ★, PS-7; heating rate = 0.4°C/min)

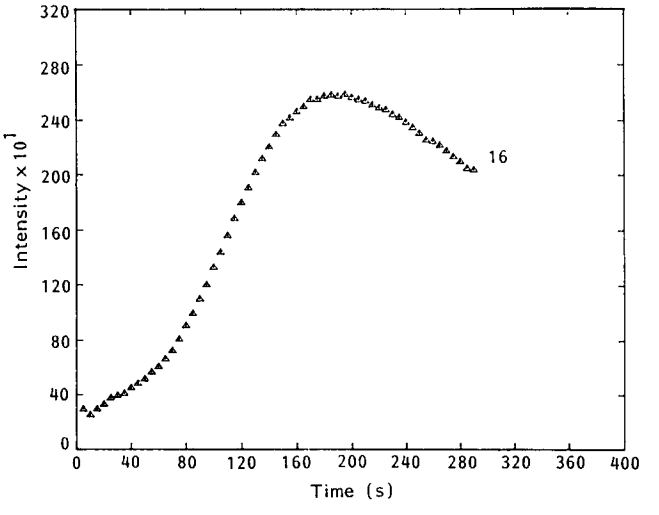

Figure 10 A typical plot of intensity against time for TMPC/PS-5 (50/50) at 242°C ($Q = 9.55 \times 10^{-3}$ Å)

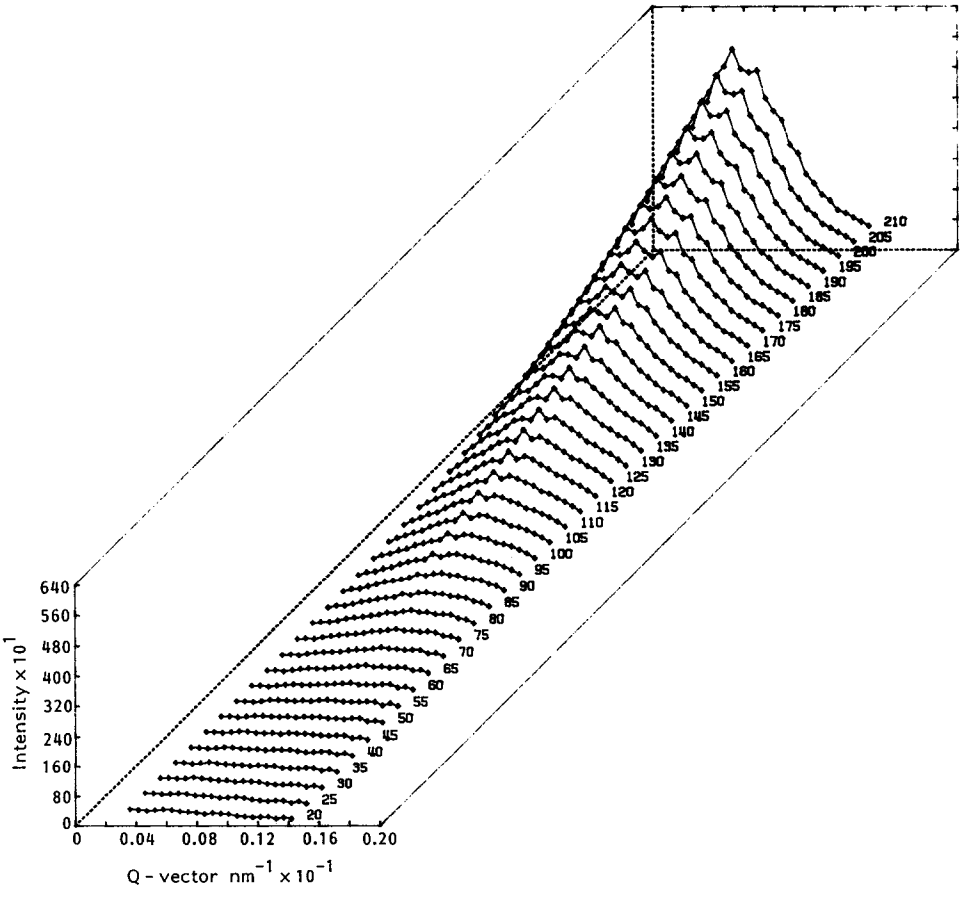

Figure 9 A typical series of $I(Q)$ plots at different times within the spinodal for TMPC/PS-5 (50/50) mixture at 242°C

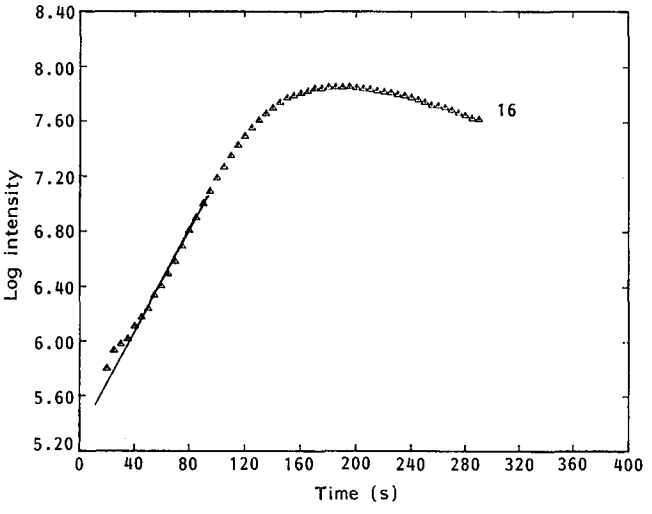

Figure 11 A plot of ln(intensity) against time for the data shown in *Figure 10*

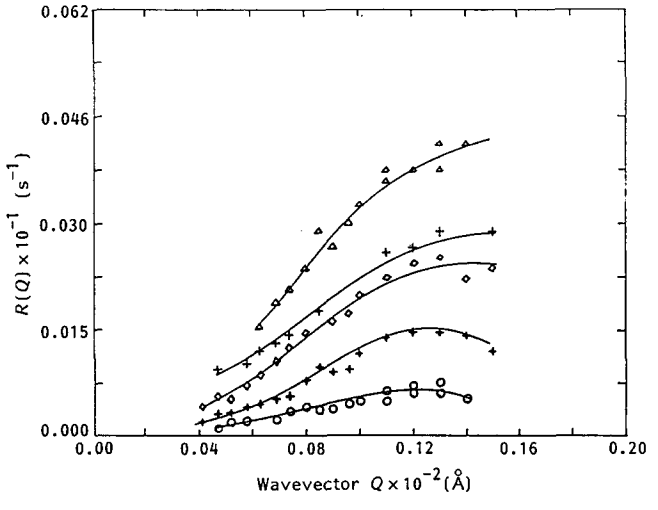

Figure 12 Plots of growth rate $R(Q)$ against Q for TMPC/PS-5 (50/50) mixture at different temperatures. ○, 234°C; ◆, 236°C; ◇, 238°C; +, 240°C; △, 242°C

Table 2 Kinetic data[a]

T (°C)	D_{app} (cm^2/s) 10^{-15}	Q_m (cm^{-1}) 10^5	D (cm) 10^{-5}	Q'_m (cm^{-1}) 10^5	Q_c (cm^{-1}) 10^5
234	1.52	1.25	5.02	1.71	2.42
236	3.44	1.30	4.83	1.57	2.22
238	6.62	>1.30	4.83	1.51	2.14
240	8.30	>1.30	4.83	1.26	1.78
242	12.1	>1.30	4.83	1.31	1.85

[a] The mixture is TMPC/PS-5 50/50

The validity of the Cahn–Hillard theory is also tested via the linear dependence of $R(Q)/Q^2$ on Q^2 predicted by equation (4). For all the data reported here linearity was observed which again supports the application of linear Cahn–Hillard theory[15]. From the intercepts of plots shown in *Figure 13* values of the Cahn–Hillard diffusion coefficient D_{app} are obtained. From the slopes of such plots together with the intercepts a second value of Q_m can be calculated which gives an internal consistency check on the use of the Cahn–Hillard theory. These data are listed as Q'_m in *Table 2*. It is obvious that although the values agree well with Q_m in the order of magnitude, they show a weak reverse temperature dependence.

As the thermodynamic force decreases, D_{app} should tend to zero at the spinodal. This is shown in *Figure 14*. Here again a good linearity was also found and the extrapolated value of T_s (233°C) agrees well with the cloud point at zero heating rate shown in *Figure 6*.

The Cahn–Hillard theory also predicts a cutoff wave vector Q_c where the $R(Q)$ equals zero. Because this value is difficult to obtain experimentally we have calculated the Q_c from the $R(Q)/Q^2$ against Q^2 plot when $R(Q)/Q^2 = 0$. These values are listed in *Table 2*. The ratio of Q_c/Q_m is obviously not in agreement with the predicted value of 1.414.

DISCUSSION

According to the Cahn–Hillard theory the following predictions can be summarized:

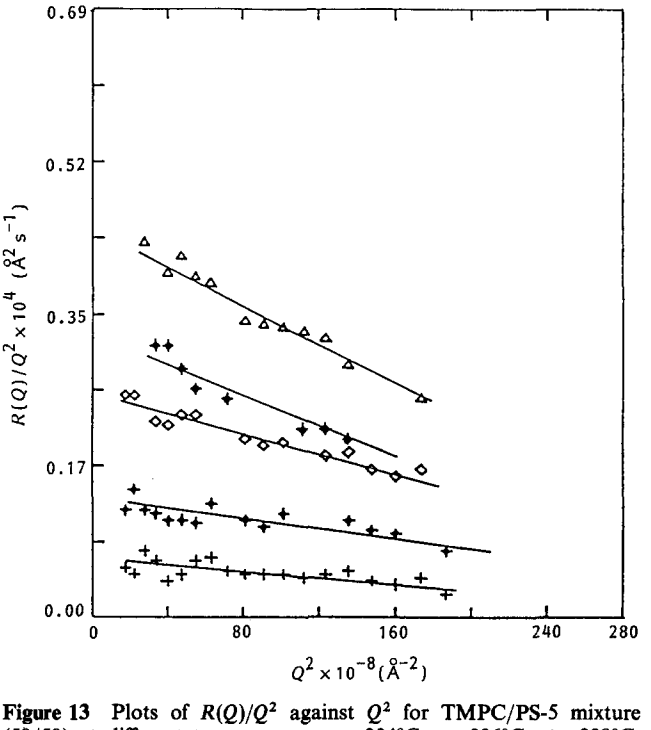

Figure 13 Plots of $R(Q)/Q^2$ against Q^2 for TMPC/PS-5 mixture (50/50) at different temperatures. +, 234°C; ◆, 236°C; ◇, 238°C; ★, 240°C; △, 242°C

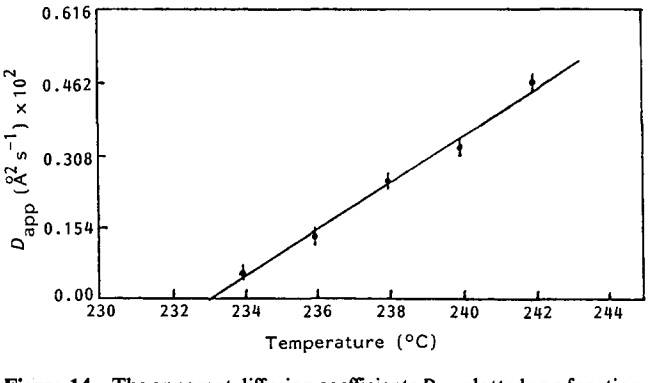

Figure 14 The apparent diffusion coefficients D_{app} plotted as a function of temperature for TMPC/PS-5 (50/50) mixture

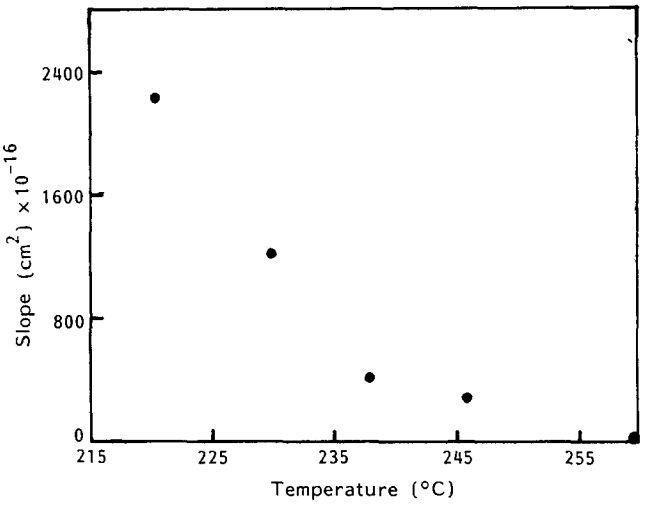

Figure 15 Plot of intercepts ($\partial^2G/\partial\phi^2$) against temperature obtained from Brereton's results

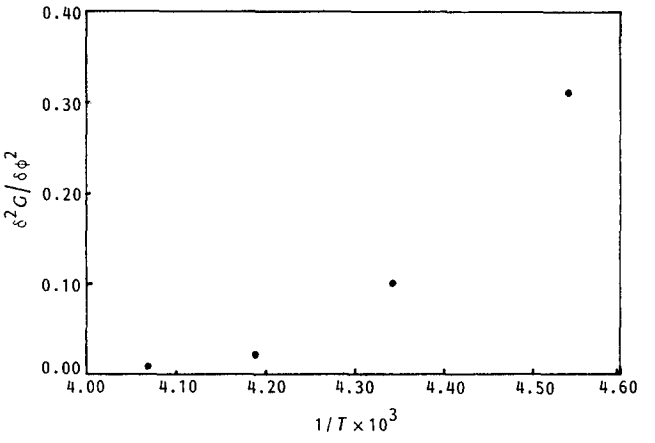

Figure 16 Plot of slopes ($=2K$) against temperature obtained from Brereton's results

(1) Intensity increases exponentially with time with a growth rate $2R(Q)$.
(2) $I(Q)$ and $R(Q)$ have maxima at

$$Q_m = \frac{1}{2}\left(-\frac{\partial^2 G}{\partial\phi^2}\Big/ K\right)^{1/2}$$

(3) $R(Q)/Q^2$ varies linearly with Q^2. The intercept is $D = -M\dfrac{\partial^2 G}{\partial\phi^2}$ and the slope is $-2MK$ so that $Q_m = (-\text{intercept}/2 \times \text{slope})^{1/2}$.
(4) The intensity does not grow above a cutoff $Q_c = (2)^{1/2}Q_m$.

The data reported here are in good agreement with the first two of these predictions, but while $R(Q)/Q^2$ does apparently vary linearly with Q^2, values of Q_m obtained from slopes and intercepts neither agree with those observed directly in $R(Q)$ nor show the correct temperature dependence. Nor, moreover, is $Q_c = (2)^{1/2}Q_m$. Such discrepancies with the simple Cahn–Hillard theory are usually attributed to several factors[5,19], such as the contribution from thermal fluctuation[5,6], and the neglect of the non-linear terms in the Cahn–Hillard theory[20,21].

Because a temperature jump cannot be instantaneous in reality, Carmesin *et al.*[7] explored the effect of a non-instantaneous temperature jump via computer simulations, and found dramatic deviations from the Cahn–Hillard behaviour which included non-linear $R(Q)/Q^2$ plots. Experimentally we also noticed a similar effect for low pre-heating temperatures (long jumps). The plots reported here for short T-jumps, however, are linear which may indicate that it is not the rate of temperature quenching which is causing the problem.

The peculiar behaviour of the interaction between TMPC and PS observed in Brereton's experiment[13] also causes concern. By extrapolating Brereton's results we have calculated the thermodynamic driving force $\partial^2G/\partial\phi^2$ at different temperatures (shown in *Figure 15*) as well as K values (shown in *Figure 16*) from the slopes and the intercepts of $S(Q)$ against Q plots. The relevant equation from reference 13 is:

$$1/S(Q) = 2(x_s - x_f) + Q^2l^2 = \partial^2G/\partial\phi^2 + 2KQ^2 \qquad (7)$$

Clearly, as noted by the authors the $\partial^2G/\partial\phi^2$ *versus* temperature plot is not linear, contrary to previous observations for other systems[8,23]. Due to this, it is not possible to extrapolate the $\partial^2G/\partial\phi^2$ from the one-phase region to the two-phase region although such values would be of great use in interpreting the disagreements between the experimental results and the simple Cahn–Hillard theory. However, looking at the trends of the data in *Figures 15* and *16* it is likely that both K and $\partial^2G/\partial\phi^2$ will further decrease as the temperature increases. Because the Q_m is proportional to the absolute value of $\partial^2G/\partial\phi^2$ (equation 4) and inversely proportional to K, a decrease of Q_m with increasing temperature, as we have seen from column 5 in *Table 2*, cannot be expected. Only if K starts to increase with T could the observed behaviour be accounted for. Thus the peculiar interaction between the two components is apparently not the cause of the disagreements shown in *Table 2*.

The neglect of the non-linear term in Cahn–Hillard theory and the effect of thermal fluctuation have been dealt with recently by Higgins *et al.*[22]. Here it was shown that discrepancies such as observed here with simple Cahn–Hillard theory could be explained by the inclusion of thermal fluctuations in the equations. Further experiments in both the one-phase and two-phase region are needed to clarify the observed behaviour in the present case.

CONCLUSIONS

Clear evidence of spinodal decomposition has been observed in the TMPC/PS blends. The Cahn–Hillard theory qualitatively predicts the behaviour of the spinodal decomposition in the early stages. Extra factors such as the effect of thermal fluctuation should be included in the treatment of the spinodal decomposition for TMPC/PS blends. The interactions between the components in the blend must be fully understood in order to resolve the problems.

ACKNOWLEDGEMENTS

TMPC was kindly supplied by BASF, West Germany.

REFERENCES

1 Olabisi, O., Robeson, L. M. and Shaw, M. T. 'Polymer–Polymer Miscibility', Academic Press, New York, 1979
2 Paul, D. R. and Newman, S., eds. 'Polymer Blends', Academic Press, New York, 1978

3 Izumitani, T. and Hashimoto, T. *J. Chem. Phys.* 1985, **83**, 3694
4 Hashimoto, T., Kumaki, J. and Kawai, H. *Macromolecules* 1983, **16**, 641
5 Synder, H. L., Meakin, P. and Reich, S. *Macromolecules* 1983, **16**, 757
6 Okada, M. and Han, C. C. *J. Chem. Phys.* 1986, **85**, 5317
7 Carmesin, H. D., Heerman, D. W. and Binder, K. *Z. Physik* 1986, **B-65**, 89
8 Higgins, J. S., Fruitwala, H. and Tomlins, P. E. *Makromol. Chem., Macromol. Symp.* 1988, **16**, 313
9 Shaw, M. T. *J. Appl. Polym. Sci.* 1974, **18**, 449
10 Casper, R. and Morbitzer, L. *Makromol. Chem.* 1977, **58/59**, 1
11 Yee, A. F. and Maxwell, M. A. *J. Macromol. Sci. Phys.* 1980, **17**, 543
12 Fernandes, A. C., Barlow, J. W. and Paul, D. R. *Polymer* 1986, **27**, 1789
13 Brereton, M. G. *et al. J. Chem. Phys.* 1987, **10**, 6144
14 Flory, P. J. *J. Chem. Phys.* 1941, **9**, 660
15 Cahn, J. W. *Trans. Met. Soc. AIME* 1968, **242**, 169
16 Schichtel, T. E. and Binder, K. *Macromolecules* 1987, **20**, 1671
17 Guo, W. *PhD Thesis* 1989, Imperial College, London, in preparation
18 Fox, T. G. *Bull. Am. Phys. Soc.* 1956, **2**, 123
19 Binder, K. Lecture notes
20 Binder, K. *J. Chem. Phys.* 1983, **79**, 6387
21 Synder, H. L. and Meakin, P. *J. Polym. Sci. Symp.* 1985, **73**, 217
22 Cook, H. E. *Acta Metall.* 1970, **18**, 297
23 Higgins, J. S., Fruitwala, H. and Tomlins, P. E. *Macromolecules* 1989, **22**, 3674